Cerebral Cortex July 2013;23:1715–1723
doi:10.1093/cercor/bhs167
Advance Access publication June 12, 2012

Less Efficient Information Transfer in Cys-Allele Carriers of *DISC1*: A Brain Network Study Based on Diffusion MRI

Yonghui Li[1,2], Bing Liu[1], Bing Hou[1], Wen Qin[3], Dawei Wang[3], Chunshui Yu[3] and Tianzi Jiang[1,2,4]

[1]LIAMA Center for Computational Medicine, National Laboratory of Pattern Recognition, Institute of Automation, Chinese Academy of Sciences, Beijing, China, [2]Queensland Brain Institute, The University of Queensland, Brisbane, Australia, [3]Department of Radiology, Tianjin Medical University General Hospital, Tianjin 300052, China and [4]Key Laboratory for NeuroInformation of Ministry of Education, School of Life Science and Technology, University of Electronic Science and Technology of China, Chengdu 610054, China

Y.L., B.L. and B.H. contributed equally to this work and should be considered as co-first authors.

Address correspondence to: Tianzi Jiang, LIAMA Center for Computational Medicine, National Laboratory of Pattern Recognition, Institute of Automation, Chinese Academy of Sciences, Beijing 100190, China. Email: jiangtz@nlpr.ia.ac.cn

Previous neuroimaging studies of brain networks have revealed less efficient information transfer in patients with schizophrenia. However, the underlying genetic basis remains largely unexplored. In this study, we investigated the brain anatomical networks of 278 healthy volunteers with different genotypes in the common missense variant (Ser704Cys) of the Disrupted-in-Schizophrenia-1 (*DISC1*) gene, which is one of the main susceptibility genes of schizophrenia and other psychiatric disorders. The anatomical brain network for each individual was constructed using fiber tractography technique based on diffusion magnetic resonance imaging (dMRI). The properties of this network were then calculated using graph theory. This revealed that Cys-allele carriers showed significantly lower global efficiency of their brain networks than Ser homozygotes, thereby supporting our hypothesis that genetic variation in *DISC1* may relate to the risk of schizophrenia by affecting the efficiency of brain network. Additional dMRI analyses were also performed at different levels, with a convergent trend towards decreased white matter integrity being consistently observed in Cys-allele carriers. Together these findings not only provide new clues for understanding *DISC1* function, but also suggest that network analyses based on graph theory combined with neuroimaging techniques may reveal structural disruptions related to genetic risk in the brains of healthy individuals.

Keywords: fiber tractography, gene, neuroimaging, schizophrenia, white matter

Introduction

In recent years there has been an explosion of studies, which viewed the human brain as a complex network and explored it utilizing graph theory analysis based on a variety of neuroimaging techniques. These investigations have consistently reported non-trivial topological properties of the human brain network, such as small-worldness, which reflect the nature of efficient information transfer (Bullmore and Sporns 2009). In particular, an increasing number of brain network studies in schizophrenia using functional and structural imaging methods have revealed not only less efficient information transfer in affected patients, but also an association between disrupted brain network properties and clinical features such as illness duration (Micheloyannis et al. 2006; Liu et al. 2008; Bassett et al. 2009; Skudlarski et al. 2010; van den Heuvel et al. 2010; Zalesky et al. 2011). However, the genetic basis underlying the less efficient organization of the brain network in schizophrenia remains largely unknown.

Disrupted-in-Schizophrenia-1 (*DISC1*) is one of the main susceptibility genes in schizophrenia and other psychiatric disorders (Callicott et al. 2005; Brandon and Sawa 2011; Johnstone et al. 2011). Despite inconsistencies across different populations (Mathieson et al. 2012), it has been widely reported that the common missense variant Ser704Cys (rs821616) in the *DISC1* gene is associated with schizophrenia (Callicott et al. 2005; DeRosse et al. 2007; Qu et al. 2007), suggesting that genetic variation may be associated with the disrupted organization of the patient's brain. *DISC1* is involved in numerous neurodevelopmental processes (Brandon et al. 2009), particularly in relation to white matter development, including neurite outgrowth (Kamiya et al. 2006), myelination (Wood et al. 2009), and axon guidance (Chen et al. 2011). Considering that white matter abnormalities and their high heritability in schizophrenia have been identified by previous studies (Hulshoff Pol et al. 2006; Sussmann et al. 2009), we considered that it would be of great interest to investigate whether such differences exist between healthy subjects with different *DISC1* genotypes. In particular, we hypothesized that the variation of Ser704Cys in *DISC1* could affect the efficient transfer of information in the brain networks of healthy subjects. This, in turn, could relate to the risk of developing schizophrenia, considering that white matter connectivity underlying the anatomical brain network has been shown to be associated with the efficient organization of the brain in previous studies utilizing diffusion magnetic resonance imaging (dMRI)-based methods in healthy and clinical populations (He and Evans 2010).

To test our hypothesis, we recruited 323 healthy Chinese young adults to our current study. The whole brain anatomical network for each individual was constructed using automated anatomical labeling (AAL) and probabilistic fiber tractography methods based on relatively high angular resolution dMRI data. The topological properties of the brain network, which were calculated using graph theory, were compared between the Cys-allele carriers and Ser homozygotes. More comprehensive analyses based on dMRI were performed at different levels to provide complementary support for our brain network findings.

Materials and Methods

Subjects

We recruited 323 healthy subjects (157 males and 166 females, mean age = 22.7 years, range = 18–31 years) to the study by advertisement.

Exclusion criteria included a history of neurological and psychological diseases in the subjects or their first-degree relatives, notable malformation, traumatic brain injury, hypothyroidism or other disorders known to be associated with mental retardation. Subjects with visible brain lesions on conventional magnetic resonance images were also excluded from the study. All subjects were examined using the Chinese Revised Wechsler Adult Intelligence Scale (WAIS-RC) (Gong 1982), except that one did not come back for the IQ test. Across all those subjects who participated, the mean full scale IQ (FSIQ) score was 116.7 (range = 70–139). All subjects were right-handed and Han Chinese in origin.

Ethics Statement

After a full explanation, all subjects gave written informed consent according to the standards set by the Ethical Committee of Tianjin Medical University.

DNA Extraction and DISC1 Ser704Cys Genotyping

We extracted genomic DNA from whole blood using EZgene™ Blood gDNA Miniprep Kit (Biomiga Inc, San Diego, CA, United States of America). We then genotyped *DISC* Ser704Cys (rs821616) in the 314 subjects using the PCR and ligation detection reaction (LDR) method (Thomas et al. 2004; Yi et al. 2009) with technical support from the Shanghai Biowing Applied Biotechnology Company.

The PCR primer sequences for Ser704Cys were: forward 5′ CCTTCAAAGGGGTCTTCCTT 3′, reverse 5′ TGCCTTTGTTTCCTC TCTGTCT 3′. PCR was carried out in 20 μL volume containing 1 μL genomic DNA, 0.4 μL primer mixture, 2 μL dNTP, 0.6 μL Mg^{2+}, 2 μL buffer, 4 μL Q-Solution and 0.3 μL Taq DNA polymerase. The amplification protocol comprised an initial denaturation and enzyme activation phase at 95 °C for 15 min followed by 35 cycles of denaturation at 94 °C for 30 s, annealing at 59 °C for 1 and 30 s, extension at 72 °C for 1 min, and then a final extension at 72 °C for 7 min. PCR products were checked in 3% agarose gels stained with ethidium bromide to ensure the amount added in LDR.

Three probes, including one common probe (rs821616_modify: P-GCCTACAGCTCCAGGAAGCCAGGGGTTTTTTTTTTTTTTTTT-FAM) and 2 discriminating probes for the 2 alleles (rs821616_A: TTTT TTTTTTTTTTTTTGAAGCTTGTCGATTGCTTATCCAGT; rs821616_T: TTTTTTTTTTTTTTTTTTTTGAAGCTTGTCGATTGCTTATCCAGA), were designed for the LDR reactions. These reactions were carried out in a 10 μL mixture containing 1 μL buffer, 1 μL probe mix, 0.05 μL Taq DNA ligase, 1 μL PCR product and 6.95 μL deionized water. The reaction program involved an initial heating at 95 °C for 2 min followed by 35 cycles of 30 s at 94 °C and 2 min at 50 °C. Reactions were stopped by chilling the tubes in an ethanol–dry ice bath and adding 0.5 mL of 0.5 mM EDTA. Aliquots of 1 μL of the reaction products were mixed with 1 μL of loading buffer (83% formamide, 8.3 mM EDTA and 0.17% blue dextran) and 1 μL ABI GS-500 Rox-Fluorescent molecular weight marker denatured at 95 °C for 2 min, and chilled rapidly on ice prior to being loaded on a 5 M urea-5% polyacrylamide gel and electrophoresed on an ABI 3100 DNA sequencer at 3000 V. Fluorescent ligation products were analyzed and quantified using the ABI GeneMapper software.

Nine subjects without *DISC1* Ser704Cys genotype data were excluded from the current study, leaving 314 subjects in total. The distribution of the *DISC1* genotype in our samples (SerSer: $N = 218$, SerCys: $N = 86$, CysCys: $N = 10$) did not significantly deviate from the Hardy–Weinberg equilibrium ($P = 0.67$).

MRI Data Acquisition and Preprocessing

DMRI images of the 314 subjects were obtained on a Signa HDx 3.0 T MR scanner (GE Medical Systems). A single shot echo planar imaging sequence (TR = 10 000 ms, TE = 64.2 ms) was employed. Diffusion sensitizing gradients were applied along 55 non-collinear directions ($b = 1000$ s/mm^2), together with 3 non-diffusion-weighted acquisitions ($b = 0$ s/mm^2) which were then averaged to generate 1 b0 image for a better signal to noise ratio. From each subject, 45 axial slices were collected. The field of view was 256 × 256 mm, the acquisition matrix was 128 × 128, the number of excitations was 1, and the slice thickness was 3 mm with no gap, which resulted in a voxel-dimension of 2 × 2 × 3 mm.

The dMRI data were visually inspected by 2 radiologists for apparent artifacts arising from subject motion and instrument malfunction. A further 36 subjects were excluded because of bad imaging quality. Eventually, 278 subjects were included for subsequent analyses, including 80 Cys-allele carriers (SerCys: $N = 72$, CysCys: $N = 8$) and 198 Ser homozygotes. The distribution of the *DISC1* genotype in these 278 subjects did not significantly deviate from the Hardy–Weinberg equilibrium ($P = 0.63$). Distortions in the dMRI images caused by eddy currents and simple head movements were then corrected by FMRIB's Diffusion Toolbox (FSL 4.1.4; http://www.fmrib.ox.ac.uk/fsl). After correction, 3D maps of the diffusion tensor and the fractional anisotropy (FA) values were calculated using FSL.

Group Characteristics Analyses

A χ^2-test was used for gender, and independent 2-sample *t*-tests were used for age, FSIQ and years of education between the 2 genotype groups. As shown in Table 1, no significant difference was found between the 2 groups.

Brain Anatomical Network Analyses

Definition of Network Node

First, we employed the AAL template (Tzourio-Mazoyer et al. 2002) available with the MRIcro software (http://www.sph.sc.edu/comd/rorden/mricro.html) to segment the cerebral cortex of each subject into 90 regions (45 for each hemisphere with the cerebellum excluded), each representing a node of the network. The parcellation process for each subject was conducted in the dMRI native space (Gong, He, et al. 2009). In detail, each individual b0 image was normalized to the EPI template in Montreal Neurological Institute (MNI) space. The resulting inverse transformation was then used to warp the AAL template from MNI space to the dMRI native space in which the discrete labeling values were preserved by using a nearest-neighbor interpolation method (Gong, He, et al. 2009). Both the normalization and the inverse transformation were implemented using the SPM8 package (http://www.fil.ion.ucl.ac.uk/spm).

Construction of the Binary Network for an Individual Brain

We performed probabilistic fiber tractography between each pair of the 90 AAL regions in every subject to estimate the connectivity between node regions. We first estimated the local probability distribution of fiber direction at each voxel using the Bayesian framework proposed by Behrens, Woolrich, et al. (2003), and a computation model capable of automatically estimating 2 fiber population within each voxel was employed (Behrens et al. 2007). Probabilistic tractography was applied by sampling 5000 streamlines per voxel. For each sampled fiber line, we drew a sample direction from the local distribution of fiber direction and then proceeded a fixed distance of 0.5 mm along this direction to a new position from which another sample direction was drawn. This propagation procedure stopped if the brain surface was reached or the fiber path looped back on itself.

Table 1
Statistical analyses on group characteristics between Ser homozygotes and Cys-allele carriers

Characteristics	Value, group mean (SD)		*P*-value
	SerSer ($n = 198$)	Cys-allele ($n = 80$)	SerSer versus Cys-allele
Gender	94 M / 104 F	32 M / 48 F	0.257
Age	22.77 (2.502)	23.09 (2.189)	0.326
FSIQ	116.84 (9.822)	117.41 (8.138)	0.647
Education	15.61 (2.513)	15.54 (3.035)	0.851

Note: For gender, we used a χ^2-test. Two-sample *t*-tests were used for age, FSIQ and education.
Abbreviations: SD, standard deviation; M, male; F, female; FSIQ, full scale IQ.

Therefore, the connectivity from a seed voxel i to another target voxel j was defined as the number of fibers passing through voxel j divided by the total number of fibers sampled from voxel I (Behrens et al. 2007). The idea of connectivity between voxels can easily be extended to the regional level. For a seed region with n voxels, 5000*n fibers were sampled (5000 fibers for each voxel). The number of fibers passing through a given region divided by 5000*n is defined as the connectivity from the seed region to this target region (Behrens et al. 2007). It should be noted that the connectivity from i to j is not necessarily equivalent to the one from j to i because the tractography results are dependent on different seeding locations. However, it has been demonstrated in a previous study that these 2 connectivity values are highly correlated with each other (Gong, Rosa-Neto, et al. 2009). The connectivity between the seed region i and the target region j is defined by averaging the 2 connectivity values. The connectivity demonstrated herein, which was derived from probabilistic tractography based on dMRI, has been widely applied and is supported by previous human brain studies (Behrens, Johansen-Berg, et al. 2003; Johansen-Berg et al. 2004; Johansen-Berg et al. 2005; Gong, Rosa-Neto, et al. 2009). The above-mentioned estimation of fiber direction distribution, subsequent probabilistic tractography and the calculation of regional connectivity were implemented using FSL software and our in-house scripts developed in the Matlab 7.8 platform.

According to the nature of the probabilistic tractography we employed in our study, the probability of connectivity we measured represents the reliability that white matter fiber tracts exist between the 2 regions (Behrens, Woolrich, et al. 2003; Behrens et al. 2007). However, there is always a risk that some false-positive connections could be included due to the limited dimensional and angular resolution of the dMRI data. To address this issue, a threshold value for the probability of connectivity was utilized to exclude connections between regions that are unlikely to be of certain validity. On the other hand, some false-negative connections (that is, connections that are real, but are rejected as false) might be excluded when a relatively large threshold value is used. Based on the findings from a similar previous study, a threshold range between 0.01 and 0.1 should be able to maximize the inclusion of real regional connections while minimizing the number of false connections (Gong, Rosa-Neto, et al. 2009). We tested this by implementing different threshold values ranging from 0.01 to 0.5 at intervals of 0.0025 and, in accordance with previous reports, found 0.1 to be the maximum threshold, which would maintain full connectivity across all 90 AAL regions in our population of 278 healthy young adults. Eventually, a 90×90 binary symmetric connectivity matrix was obtained for each subject using the above procedures, in which the x- and y-axes corresponded to the 90 AAL regions and the value of each entry in this matrix was either 0, indicating that no connection existed between the corresponding pair of brain regions, or 1, indicating that the 2 regions were connected in the particular subject.

Graph Theoretical Analyses of the Network Topological Properties

A complex network can be represented as a graph in which nodes correspond to the elements of the system and arcs to the interactions between them (Boccaletti et al. 2006). In the current study, we investigated a binary anatomical network G_B, which modeled the anatomical connections between different cortical and subcortical AAL regions for each individual brain. Several topological properties were included for our investigations:

1. We used N to represent the total number of nodes in the network.
2. We used E to represent the total number of edges in the network.
3. The subgraph G_i is defined as the set of nodes that are the direct neighbors of the ith node. The degree of each node $D_{i,i=1,2,\ldots,90}$ is defined as the number of nodes in G_i. The degree of the network is the average across all the nodes in the graph:

$$D_p = \frac{1}{N}\sum_{i \in G} D_i.$$

1. The absolute clustering coefficient of a node C_i is defined as the ratio of the number of existing connections to the number of all possible connections in the subgraph G_i:

$$C_i = \frac{E_i}{D_i(D_i - 1)/2}$$

in which E_i is the number of edges in G_i (Watts and Strogatz 1998; Strogatz 2001). The absolute clustering coefficient of the network is the average of all nodes:

$$C_p = \frac{1}{N}\sum_{i \in G} C_i,$$

which is a measure of the extent of local cliquishness or local efficiency of information transfer of a network (Watts and Strogatz 1998; Latora and Marchiori 2001).

1. The mean shortest absolute path length of a node is defined as

$$L_i = \frac{1}{N-1}\sum_{\substack{i,j \in G_w \\ i \neq j}} d_{ij}$$

in which d_{ij} is the shortest absolute path length between the i and j nodes. For a binary network, the length of every edge is 1, and d_{ij} is defined as the number of edges along the shortest path connecting nodes i and j. The mean shortest absolute path length of the network is the average across all nodes

$$L_p = \frac{1}{N}\sum_{i \in G} L_i,$$

which quantifies the extent of average connectivity or the overall routing efficiency of the network (Achard and Bullmore 2007).

1. The global efficiency of the network E_{glob} is defined as

$$E_{glob} = \frac{1}{N(N-1)}\sum_{\substack{i,j \in G \\ i \neq j}} \frac{1}{d_{ij}},$$

which is the inverse of the harmonic mean of the minimum absolute path length between each pair of nodes, reflecting the global efficiency of parallel information transfer in the network (Latora and Marchiori 2001; Achard and Bullmore 2007).

Two-sample t-tests on the properties of binary networks were performed between the 2 genotype groups using SPSS13.0. We included gender, age, FSIQ and education duration of the subjects as covariates in order to exclude their potential influence. The threshold value was set at $P < 0.05$ (FWE-corrected) for significance.

Comprehensive Analyses Based on dMRI at Different Levels

More comprehensive analyses based on dMRI were performed at different levels to further explore the white matter differences between the 2 genotype groups in order to provide more support for our brain network analyses.

Voxel-based Analysis of FA Images

Utilizing the SPM8 package, each subject's b0 image was first normalized to the EPI template in MNI space. The normalization consisted of a 12 iteration linear transformation and a non-linear transformation with $7 \times 8 \times 7$ basis functions. Parameters from this transformation were then applied to each subject's FA image, while re-sampling the volume into a voxel size of $2 \times 2 \times 2$ mm. Each normalized FA image was then spatially smoothed by an 8-mm full-width at half-maximum Gaussian kernel to reduce the effect of misregistration in spatial normalization (Ashburner and Friston 2000; Jones et al. 2005).

We performed a 2-sample *t*-test on the normalized FA images between the 2 groups in a voxel-based manner, using SPM8. The threshold value was set at $P < 0.05$ (FWE-corrected) with a cluster size >30 voxels ($2 \times 2 \times 2 \times 30 = 240$ mm^3) for significance.

Regions of Interest and Fibers of Interest Analyses of FA Images

We further selected regions and fiber tracts in each individual and calculated the average FA value of each selected regions of interest (ROI) and fibers of interest (FOI) for subsequent statistical analyses.

First, we selected all 90 AAL regions as ROIs in the dMRI native space of each subject by utilizing the AAL template. Each individual b0 image had already been normalized to the EPI template in MNI space in previous analyses (see the Anatomical Network Analyses section). The resulting inverse transformation was then used to warp the AAL template from MNI space to the dMRI native space in which the discrete labeling values were preserved by using a nearest-neighbor interpolation method (Gong, He, et al. 2009). The inverse transformation was implemented using the SPM8 package. The AAL template is not a pure cortical gray matter mask but includes tissues from both cortical gray matter and subcortical white matter (Tzourio-Mazoyer et al. 2002). To address this issue, a criterion of FA ≥ 0.2 was set to restrict our analyses within the white matter tissue underlying the cortical region or adjacent to subcortical structures.

We then extracted 20 major white matter fiber tracts as FOIs in the dMRI native space of each subject by utilizing the JHU white matter tractography atlas available with FSL (Wakana et al. 2004; Hua et al. 2008), which was built on 28 normal subjects of similar age (17 males, 11 females, mean age = 29 years) to our healthy individuals. The inverse transformation was implemented using the same procedure we employed in ROI analyses with the SPM8 package.

Two-sample *t*-tests on the average FA values of the selected ROIs and FOIs were performed between the 2 genotype groups.

Results

Topological Properties of the Brain Anatomical Network

Figure 1 shows the AAL template in standard MNI space (Fig. 1*A* and *B*) and the wrapped AAL templates in the native dMRI space of 2 randomly selected subjects from the Ser homozygotes (Fig. 1*C* and *D*) and Cys-allele carriers (Fig. 1*E* and *F*). This illustrates the good quality and consistency of the transformations of the AAL template into native dMRI space that we applied across subjects. In Figure 2, examples of probabilistic fiber tractography are shown in randomly selected subjects from the 2 genotype groups. The resultant trajectories are consistent with existing anatomical knowledge (Witelson 1989) as well as with the results of a previous dMRI study (Wakana et al. 2007), thereby providing further support for the validation of our network construction. We successfully constructed binary anatomical networks for each of the final 278 subjects in the form of symmetric connectivity matrices (see Materials and Methods). Figure 3 illustrates the 3D representation of the network in anatomical space, which was obtained by averaging across the binary connectivity matrices of all 278 subjects (Fig. 3*A*–*C*). The connectivity pattern of the network is generally comparable with the results of previous studies utilizing dMRI data (Hagmann et al. 2008; Iturria-Medina et al. 2008; Gong, He, et al. 2009) as well as current anatomical knowledge (Witelson 1989; Mori et al. 2002; Wakana et al. 2007), thereby increasing the validity of our constructed network.

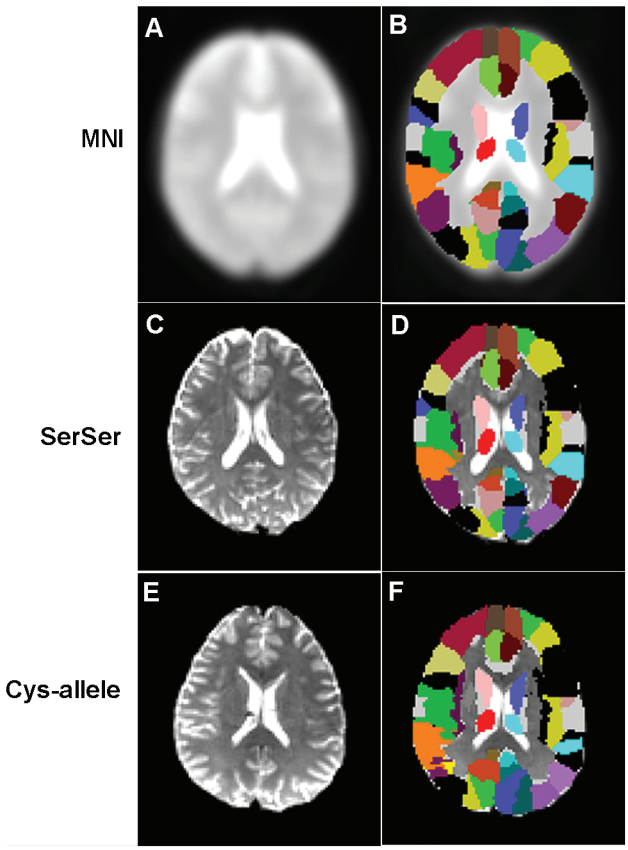

Figure 1. Examples of AAL regions wrapped into dMRI native space (*A*) EPI template in MNI space; (*B*) AAL regions overlaid on the EPI template in MNI space; (*C*) b0 image of one Ser homozygous subject; (*D*) AAL regions overlaid on the b0 image of this Ser homozygous subject; (*E*) b0 image of one Cys-allele subject; (*F*) AAL regions overlaid on the b0 image of this Cys-allele subject. Image dimensions in MNI space are $181 \times 217 \times 181$ mm with voxel dimensions of $1 \times 1 \times 1$ mm; image dimensions in native dMRI space are $128 \times 128 \times 45$ mm with voxel dimensions of $2 \times 2 \times 3$ mm. The homologous brain regions in the AAL template are coded in different colors because the areas in the left and right hemispheres were considered separately.

Different Network Properties Between Ser Homozygotes and Cys-Allele Carriers

As shown in Table 2, significant differences ($P < 0.05$, FWE-corrected) in network properties were found between the 2 genotype groups by 2-sample *t*-tests. We found that compared with Ser homozygotes, Cys-allele carriers showed significantly fewer edges (Fig. 4*A*), longer shortest path length (Fig. 4*B*), and lower global efficiency (Fig. 4*C*) of their brain anatomical networks; no significant difference in cluster coefficient (C_p) was observed between the 2 groups.

Voxel-based Analysis of FA

The FA images were compared in a voxel-wise manner by a 2-sample *t*-test between the 2 genotype groups. No significant difference of FA value was found ($P < 0.05$, FWE-corrected, cluster size >30 voxels).

Different FA Values Between Ser Homozygotes and Cys-Allele Carriers Based on ROI and FOI Analyses

As shown in Table 3, a trend towards decreased averaged FA values was observed in 2 AAL regions including Postcentral_L and Parietal_Sup_L (the names of AAL regions are provided

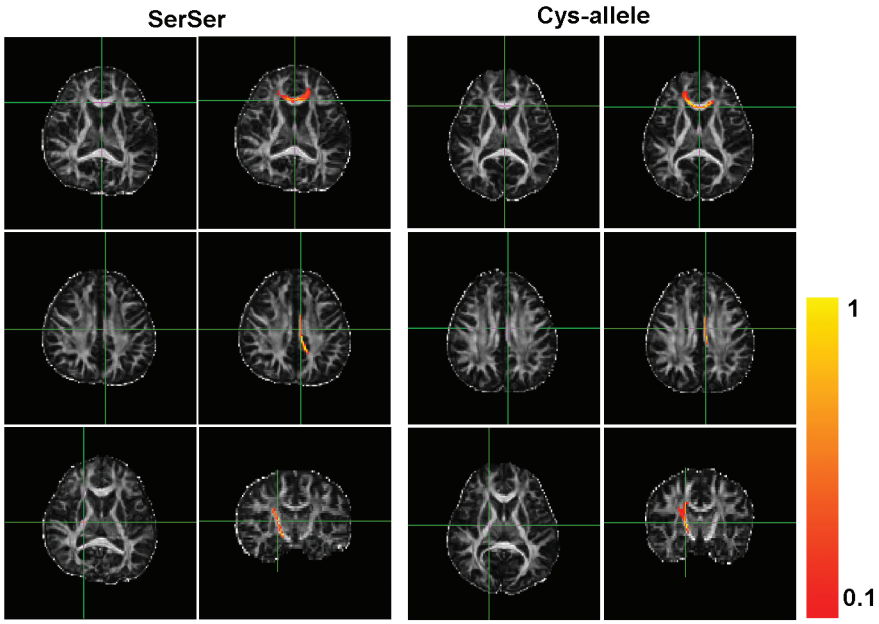

Figure 2. Examples of probabilistic fiber tractography in 2 randomly selected subjects. Columns 1 and 3: FA images of one Ser homozygote and one Cys-allele carrier, in which 3 single seed voxels were placed in the genu of the corpus callosum (row 1), the cingulum (row 2), and the corticospinal tract (row 3); the seed voxel is marked by the green cross. Columns 2 and 4: corresponding probabilistic fiber tractography results overlaid on the FA images; the color of each voxel represents the number of fibers passing through it divided by the total number of fibers sampled from the seed voxel (5000), ranging from the threshold value we used in this manuscript 0.1 (red), indicating that at least 10% of the sampled fibers passed through this voxel, to 1 (yellow), indicating that all sampled fibers passing through this voxel.

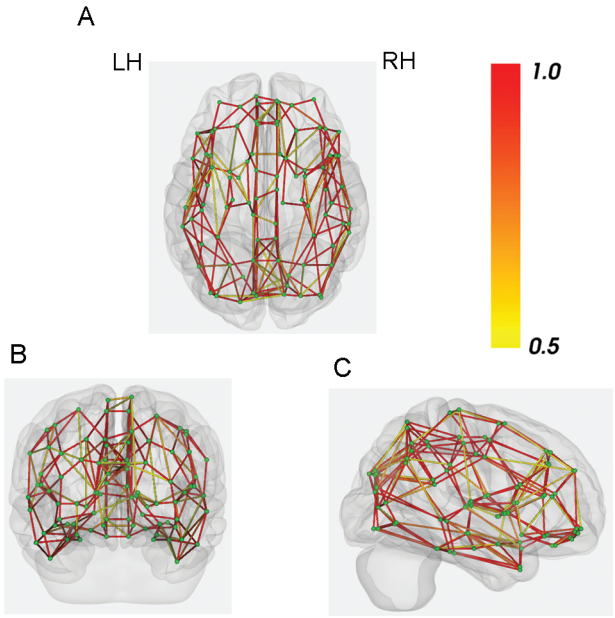

Figure 3. 3D presentation of the binary connectivity matrixes averaged across all subjects. (*A*, *B*, and *C*): A 3D presentation of the network in anatomical space, in which the green points correspond to the 90 AAL regions and the lines correspond to the connections between corresponding pairs of brain regions. The colors of the lines represent the percentage of subjects that had a connection between the corresponding pair of brain regions, ranging from 0.5 (yellow), indicating that at least half of the subjects showed a connection, to 1 (red), indicating that the 2 regions were connected in all subjects. Abbreviations: LH, left hemisphere; RH, right hemisphere.

by the MRIcro software; "L" means that the brain region is located in the left hemisphere; "R" denotes the right hemisphere) in Cys-allele carriers compared with Ser homozygotes ($P < 0.05$, uncorrected). No tendency towards higher FA value was found in the Cys-allele group compared with the Ser homozygotes.

Table 2

Two-sample *t*-tests on properties of brain anatomical networks between Ser homozygotes and Cys-allele carriers

Topological properties	Value, group mean (SD)		*P*-value (2-sample *t*-test) (equal variances assumed)
	SerSer ($n = 198$)	Cys-allele ($n = 80$)	SerSer versus Cys-allele
E	248.57 (21.013)	239.96 (22.975)	0.001*
Cp	0.414 (0.0298)	0.405 (0.0314)	0.036
Lp	3.945 (0.2338)	4.056 (0.2858)	<0.001*
E_glob	0.322 (0.0154)	0.315 (0.0178)	0.001*

Note: SD, standard deviation.

*Significance was set at $P < 0.05$ (FWE-corrected) with equal variances assumed. The results shown are under the threshold of 0.1 for probability of connectivity between regions. E, Cp, Lp and E_glob denote the number of edges, average clustering coefficient, mean shortest path length and global efficiency of the network respectively. Detailed definitions can be found in the Materials and Methods section.

Figure 5 illustrates the JHU white matter tractography atlas in standard MNI space and the wrapped templates in native dMRI space of 2 randomly selected subjects from the Ser homozygotes and Cys-allele carriers, providing support for the quality and consistency of the transformations that we applied across subjects. Two out of 20 white matter fiber tracts, including the left and right anterior thalamic radiations (the names of the FOIs are provided by the FSL software; "L" means that the brain region is located in the left hemisphere; "R" denotes the right hemisphere), displayed a lower average FA value in Cys-allele carriers than in Ser homozygotes ($P < 0.05$, uncorrected). No trend towards a higher FA value was found in the Cys-allele group compared with the Ser homozygotes.

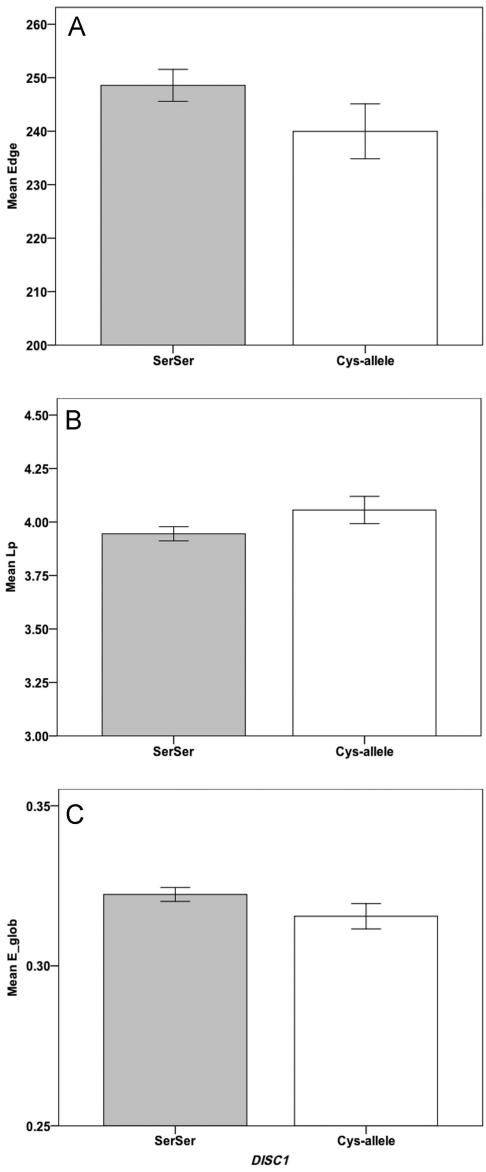

Figure 4. Disrupted properties of brain anatomical networks in Cys-allele carriers compared with Ser homozygotes. Compared with Ser homozygotes, Cys-allele carriers showed significantly fewer edges (*A*), longer shortest path length (*B*), and lower global efficiency (*C*) of their brain networks.

Discussion

In this study, we successfully constructed individual binary anatomical networks for the brains of 278 young healthy Chinese Han adults using a probabilistic fiber tractography method based on dMRI data. The topological network properties we uncovered were in accordance with the findings of previous similar human brain network studies that were done on a macro-scale utilizing dMRI (Hagmann et al. 2007, 2008; Iturria-Medina et al. 2008; Gong, He, et al. 2009; Gong, Rosa-Neto, et al. 2009; Li, Liu, et al. 2009; Shu et al. 2009; Iturria-Medina et al. 2011; Wang et al. 2012). More importantly, we found significantly lower global efficiency of the brain networks in Cys-allele carriers of *DISC1* compared with Ser homozygotes, providing direct support for our hypothesis that the variation of Ser704Cys in *DISC1* affects the efficient transfer of information in the brain networks of healthy subjects. To the best of our knowledge, this is the first study that has investigated the association between *DISC1* and brain anatomical networks in healthy individuals using a dMRI-based method. Our findings suggest that the topological properties of brain networks are modulated by genes that may relate to the development of psychiatric disorders.

Non-invasive mapping of anatomical networks in the human brain at the individual level has been facilitated by recent advances in dMRI-based tractography techniques (Hagmann et al. 2007, 2008; Iturria-Medina et al. 2008; Gong, He, et al. 2009; Gong, Rosa-Neto, et al. 2009; Li, Liu, et al. 2009; Shu et al. 2009; Iturria-Medina et al. 2011; Wang et al. 2012). In particular, disrupted anatomical network properties have been revealed by several recent studies of schizophrenia, suggesting less efficiency of brain structural organization in clinical cohorts. In the study of Skudlarski et al. (2010), functional and anatomical connectivity maps were constructed for 27 schizophrenia patients, showing reduced coherence between functional and structural modalities compared with 27 normal controls. In the work of van den Heuvel et al. (2010), weighted structural networks of 40 schizophrenia patients and 40 healthy controls were established using methods based on diffusion and structural MRI techniques, revealing reduced global efficiency of frontal, temporal, and occipital brain regions in the former group. In another study conducted by Zalesky et al. (2011), binary brain networks were constructed for 74 chronic schizophrenia patients and 32 control subjects using deterministic tractography method,

Table 3
ROIs and FOIs with different average FA values in Ser homozygotes and Cys-allele carriers

	FA, group mean (SD)		*P*-value (2-samples *t*-test) (equal variances assumed)
	SerSer ($n = 198$)	Cys-allele ($n = 80$)	SerSer versus Cys-allele
ROIs			
Postcentral_L	0.3897 (0.0134)	0.3858 (0.0128)	0.018*
Parietal_Sup_L	0.3781 (0.0197)	0.3723 (0.0181)	0.013*
FOIs			
Anterior_thalamic_radiation_L	0.3590 (0.0281)	0.3485 (0.0431)	0.029* (equal variances not assumed)
Anterior_thalamic_radiation_R	0.3465 (0.0291)	0.3373 (0.0381)	0.021*

Note: ROI, regions of interest; FOI, fibers of interest; FA, fractional anisotropy; SD, standard deviation.
*The threshold value was set at $P < 0.05$ (uncorrected).

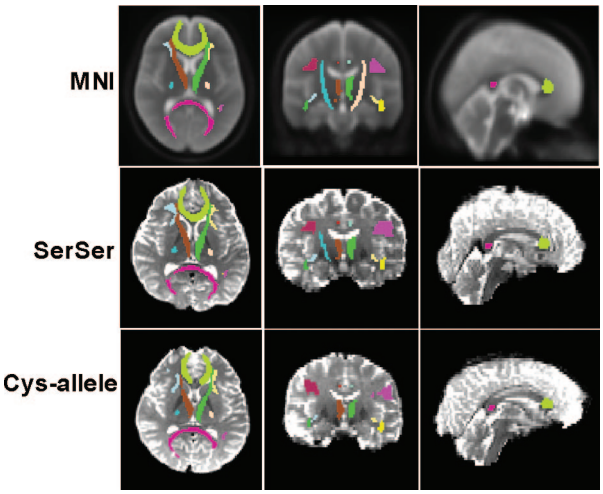

Figure 5. Examples of FOI wrapped into dMRI native space. Row 1: JHU white matter tractography atlas in MNI space onverlaid on the JHU-ICBM-T2 template; Row 2: FOI overlaid on the b0 image of one randomly selected Ser homozygote; Row 3: FOI overlaid on the b0 image of one randomly selected Cys-allele carrier.

demonstrating widespread dysconnectivity in white matter connectional architecture in the patient group. These schizophrenia patient results reflect our current findings in healthy young adults, in whom significantly different network properties were found to be associated with the common missense Ser704Cys variant of *DISC1* (Callicott et al. 2005).

DISC1 is involved in multiple processes in white matter development, including neurite outgrowth (Kamiya et al. 2006), myelination (Wood et al. 2009), and axon guidance (Chen et al. 2011). For example, knock-down of *DISC1* function in zebra fish leads to severe disruption of axonal development (Brandon et al. 2009). One recent study (Singh et al. 2011) also reported that the *DISC1* Ser704Cys variant inhibits migration of neurons in the developing neocortex, which may be a possible mechanism for its role in neuropsychiatric phenotypes. Although there are inconsistencies in their results, various studies have suggested that Ser704Cys has an impact on the risk of developing psychiatric disorders (Callicott et al. 2005; DeRosse et al. 2007; Qu et al. 2007) as well as on the modulation of human brain structure and function (Callicott et al. 2005; Hashimoto et al. 2006; DeRosse et al. 2007; Di Giorgio et al. 2008; Sprooten et al. 2011). In particular, Qu et al. (2007) reported a significant positive association between the *DISC1* Cys-allele and schizophrenia in a Chinese Han population. To our knowledge, neuroimaging studies focusing on the association between the *DISC1* Ser704Cys variant and the white matter of the brain are rare. Hashimoto et al. (2006) demonstrated reduced gray matter volume in the cingulate cortex and decreased FA in prefrontal white matter of individuals carrying the Cys-allele for Ser704Cys. However, Sprooten et al. (2011) also reported significantly decreased FA across the brain in *DISC1* Ser-allele carriers compared with Cys homozygotes. In the current study, we found significantly decreased global efficiency in the brain anatomical networks of Cys-allele carriers compared with Ser homozygotes, indicating white matter integrity disruption across the brain in healthy subjects with the Cys-allele genotype. The propagation of fiber tracking which was employed in our probabilistic tractography technique depends on the white matter integrity characterized by the diffusion profile of water molecules estimated in each voxel (Mori and Zhang 2006). Therefore, the probabilistic tractography we used in this study is capable not only of partially solving the fiber-crossing issue in the human brain, due to the reasonable computing model we used as well as the relatively high angular resolution dMRI data we acquired, but also of calculating the connectivity probabilities between voxels and regions (Behrens, Johansen-Berg, et al. 2003; Behrens, Woolrich, et al. 2003; Behrens et al. 2007; Gong, Rosa-Neto, et al. 2009). Based on the nature of our probabilistic tractography, we believe that the less efficient network organization found in Cys-allele carriers indicates minor decreased white matter integrity in these subjects, which is further supported by the results of our voxel-based analysis (VBA), ROI, and FOI analyses. This leads us to speculate that the observed differences in network organization could be reflected in variations in cognitive performance, due to the relatively weak fidelity of the underlying white matter to facilitate the rapid and error-free transmission of information between different brain regions (Jung and Haier 2007). However, no significant difference in IQ performance was found between the 2 genotype groups. This phenomenon has been commonly seen in imaging genetic studies. Imaging features as an intermediate phenotype may be more sensitive and closer to the biological effect of a genetic polymorphism, compared with emergent behavioral properties, as shown in our previous study (Li, Yu, et al. 2009) and reported by other researchers (Mattay et al. 2008; Bigos and Weinberger 2010; Meyer-Lindenberg 2010).

The comprehensive analyses we performed on different levels, including VBA, ROI, and FOI, revealed no significant difference in FA between the 2 genotype groups. However, a convergent trend towards decreased FA was consistently observed in Cys-allele carriers compared with Ser homozygotes, although this effect could not survive multiple corrections in statistical analyses (Table 3). This suggests that the differences in white matter integrity between the 2 genotype groups are minor, which we believe to be reasonable, considering that all the subjects in the 2 groups were healthy individuals who were well matched in terms of gender, age, IQ, and education. On the other hand, when we viewed the brain as an integrated system by exploring the topological properties of the brain networks, such as global efficiency, we found significantly disrupted network attributes in Cys-allele carriers. Our results indicate that investigations based on whole brain network models and graph theory may be more informative when exploring the structural organization of the brain in healthy individuals, revealing disrupted attributes of the brain due to the accumulation of minor alterations in white matter integrity. The network topological properties may be plausible endophenotypes for exploring the genetic risk of psychiatric disorders.

The efficiency of information transfer that we measured in the current study, using a graph theory method based on fiber tractography of dMRI, reflects the efficiency of the macro-scale structural organization of the brain from a network point of view. This information transfer efficiency may reflect that of the brain itself, including neurotransmitter release at synapses and action potential propagation along axons. However, more comprehensive studies will be necessary to better characterize the relationship between network efficiency on a macro-scale and micro-scale signal transmission.

In conclusion, we have found significant differences in the topological properties of the anatomical brain network between healthy individuals with different *DISC1* genotypes. Cys-allele carriers showed significantly lower global efficiency of their brain networks compared with Ser homozygotes, indicating that different efficiency of information transfer in their brains could confer different genetic risk of schizophrenia in these *DISC1* genotypes. Our findings not only provide new clues for understanding *DISC1* function, but also suggest that network analyses based on graph theory combined with brain imaging techniques may help reveal potential structural disruptions related to genetic risk in the brains of healthy individuals. It should also be noted that Ser704Cys is not the only functional variation of the *DISC1* gene (Burdick et al. 2008). The effects of other functional *DISC1* single nucleotide polymorphisms (e.g. Leu607Phe) and their interactions with Ser704Cys in terms of brain networks deserve further investigation. For example, future studies of transgenic mice may provide us with a more comprehensive understanding of the association between *DISC1* and altered brain networks.

Funding

This work was partially supported by the National Key Basic Research and Development Program (973) (Grant No. 2011CB707800) and the Natural Science Foundation of China (Grant Nos. 91132301 and 81000582).

Notes

The authors thank Dr Rowan Tweedale for English-editing assistance and discussions. *Conflict of Interest*: None declared.

References

Achard S, Bullmore E. 2007. Efficiency and cost of economical brain functional networks. PLoS Comput Biol. 3:e17.

Ashburner J, Friston KJ. 2000. Voxel-based morphometry—the methods. Neuroimage. 11:805–821.

Bassett DS, Bullmore ET, Meyer-Lindenberg A, Apud JA, Weinberger DR, Coppola R. 2009. Cognitive fitness of cost-efficient brain functional networks. Proc Natl Acad Sci USA. 106:11747–11752.

Behrens TE, Berg HJ, Jbabdi S, Rushworth MF, Woolrich MW. 2007. Probabilistic diffusion tractography with multiple fibre orientations: what can we gain? Neuroimage. 34:144–155.

Behrens TE, Johansen-Berg H, Woolrich MW, Smith SM, Wheeler-Kingshott CA, Boulby PA, Barker GJ, Sillery EL, Sheehan K, Ciccarelli O *et al*. 2003. Non-invasive mapping of connections between human thalamus and cortex using diffusion imaging. Nat Neurosci. 6:750–757.

Behrens TE, Woolrich MW, Jenkinson M, Johansen-Berg H, Nunes RG, Clare S, Matthews PM, Brady JM, Smith SM. 2003. Characterization and propagation of uncertainty in diffusion-weighted MR imaging. Magn Reson Med. 50:1077–1088.

Bigos KL, Weinberger DR. 2010. Imaging genetics–days of future past. Neuroimage. 53:804–809.

Boccaletti S, Latora V, Moreno Y, Chavez M, Hwang DU. 2006. Complex networks: structure and dynamics. Phys Rep. 424:175–308.

Brandon NJ, Millar JK, Korth C, Sive H, Singh KK, Sawa A. 2009. Understanding the role of DISC1 in psychiatric disease and during normal development. J Neurosci. 29:12768–12775.

Brandon NJ, Sawa A. 2011. Linking neurodevelopmental and synaptic theories of mental illness through DISC1. Nat Rev Neurosci. 12:707–722.

Bullmore E, Sporns O. 2009. Complex brain networks: graph theoretical analysis of structural and functional systems. Nat Rev Neurosci. 10:186–198.

Burdick KE, Kamiya A, Hodgkinson CA, Lencz T, DeRosse P, Ishizuka K, Elashvili S, Arai H, Goldman D, Sawa A *et al*. 2008. Elucidating the relationship between DISC1, NDEL1 and NDE1 and the risk for schizophrenia: evidence of epistasis and competitive binding. Hum Mol Genet. 17:2462–2473.

Callicott JH, Straub RE, Pezawas L, Egan MF, Mattay VS, Hariri AR, Verchinski BA, Meyer-Lindenberg A, Balkissoon R, Kolachana B *et al*. 2005. Variation in DISC1 affects hippocampal structure and function and increases risk for schizophrenia. Proc Natl Acad Sci USA. 102:8627–8632.

Chen SY, Huang PH, Cheng HJ. 2011. Disrupted-in-Schizophrenia 1-mediated axon guidance involves TRIO-RAC-PAK small GTPase pathway signaling. Proc Natl Acad Sci USA. 108:5861–5866.

DeRosse P, Hodgkinson CA, Lencz T, Burdick KE, Kane JM, Goldman D, Malhotra AK. 2007. Disrupted in schizophrenia 1 genotype and positive symptoms in schizophrenia. Biol Psychiatry. 61:1208–1210.

Di Giorgio A, Blasi G, Sambataro F, Rampino A, Papazacharias A, Gambi F, Romano R, Caforio G, Rizzo M, Latorre V *et al*. 2008. Association of the SerCys DISC1 polymorphism with human hippocampal formation gray matter and function during memory encoding. Eur J Neurosci. 28:2129–2136.

Gong G, He Y, Concha L, Lebel C, Gross DW, Evans AC, Beaulieu C. 2009. Mapping anatomical connectivity patterns of human cerebral cortex using in vivo diffusion tensor imaging tractography. Cereb Cortex. 19:524–536.

Gong G, Rosa-Neto P, Carbonell F, Chen ZJ, He Y, Evans AC. 2009. Age- and gender-related differences in the cortical anatomical network. J Neurosci. 29:15684–15693.

Gong YX. 1982. Manual of modified Wechsler Adult Intelligence Scale (WAIS-RC) (in Chinese). Changsha, China: Hunan Med College.

Hagmann P, Cammoun L, Gigandet X, Meuli R, Honey CJ, Wedeen VJ, Sporns O. 2008. Mapping the structural core of human cerebral cortex. PLoS Biol. 6:e159.

Hagmann P, Kurant M, Gigandet X, Thiran P, Wedeen VJ, Meuli R, Thiran JP. 2007. Mapping human whole-brain structural networks with diffusion MRI. PLoS One. 2:e597.

Hashimoto R, Numakawa T, Ohnishi T, Kumamaru E, Yagasaki Y, Ishimoto T, Mori T, Nemoto K, Adachi N, Izumi A *et al*. 2006. Impact of the DISC1 Ser704Cys polymorphism on risk for major depression, brain morphology and ERK signaling. Hum Mol Genet. 15:3024–3033.

He Y, Evans A. 2010. Graph theoretical modeling of brain connectivity. Curr Opin Neurol. 23:341–350.

Hua K, Zhang J, Wakana S, Jiang H, Li X, Reich DS, Calabresi PA, Pekar JJ, van Zijl PC, Mori S. 2008. Tract probability maps in stereotaxic spaces: analyses of white matter anatomy and tract-specific quantification. Neuroimage. 39:336–347.

Hulshoff Pol HE, Schnack HG, Mandl RC, Brans RG, van Haren NE, Baare WF, van Oel CJ, Collins DL, Evans AC, Kahn RS. 2006. Gray and white matter density changes in monozygotic and same-sex dizygotic twins discordant for schizophrenia using voxel-based morphometry. Neuroimage. 31:482–488.

Iturria-Medina Y, Perez Fernandez A, Morris DM, Canales-Rodriguez EJ, Haroon HA, Garcia Penton L, Augath M, Galan Garcia L, Logothetis N, Parker GJ *et al*. 2011. Brain hemispheric structural efficiency and interconnectivity rightward asymmetry in human and nonhuman primates. Cereb Cortex. 21:56–67.

Iturria-Medina Y, Sotero RC, Canales-Rodriguez EJ, Aleman-Gomez Y, Melie-Garcia L. 2008. Studying the human brain anatomical network via diffusion-weighted MRI and Graph Theory. Neuroimage. 40:1064–1076.

Johansen-Berg H, Behrens TE, Robson MD, Drobnjak I, Rushworth MF, Brady JM, Smith SM, Higham DJ, Matthews PM. 2004. Changes in connectivity profiles define functionally distinct

regions in human medial frontal cortex. Proc Natl Acad Sci USA. 101:13335–13340.
Johansen-Berg H, Behrens TE, Sillery E, Ciccarelli O, Thompson AJ, Smith SM, Matthews PM. 2005. Functional-anatomical validation and individual variation of diffusion tractography-based segmentation of the human thalamus. Cereb Cortex. 15:31–39.
Johnstone M, Thomson PA, Hall J, McIntosh AM, Lawrie SM, Porteous DJ. 2011. DISC1 in schizophrenia: genetic mouse models and human genomic imaging. Schizophr Bull. 37:14–20.
Jones DK, Symms MR, Cercignani M, Howard RJ. 2005. The effect of filter size on VBM analyses of DT-MRI data. Neuroimage. 26:546–554.
Jung RE, Haier RJ. 2007. The parieto-frontal integration theory (P-FIT) of intelligence: converging neuroimaging evidence. Behav Brain Sci. 30:135–154; discussion 154–187.
Kamiya A, Tomoda T, Chang J, Takaki M, Zhan C, Morita M, Cascio MB, Elashvili S, Koizumi H, Takanezawa Y *et al*. 2006. DISC1-NDEL1/NUDEL protein interaction, an essential component for neurite outgrowth, is modulated by genetic variations of DISC1. Hum Mol Genet. 15:3313–3323.
Latora V, Marchiori M. 2001. Efficient behavior of small-world networks. Phys Rev Lett. 87:198701.
Li J, Yu C, Li Y, Liu B, Liu Y, Shu N, Song M, Zhou Y, Zhu W, Li K *et al*. 2009. COMT val158met modulates association between brain white matter architecture and IQ. Am J Med Genet B Neuropsychiatr Genet. 150B:375–380.
Li Y, Liu Y, Li J, Qin W, Li K, Yu C, Jiang T. 2009. Brain anatomical network and intelligence. PLoS Comput Biol. 5:e1000395.
Liu Y, Liang M, Zhou Y, He Y, Hao Y, Song M, Yu C, Liu H, Liu Z, Jiang T. 2008. Disrupted small-world networks in schizophrenia. Brain. 131:945–961.
Mathieson I, Munafo MR, Flint J. 2012. Meta-analysis indicates that common variants at the DISC1 locus are not associated with schizophrenia. Mol Psychiatry. 17:634–641.
Mattay VS, Goldberg TE, Sambataro F, Weinberger DR. 2008. Neurobiology of cognitive aging: insights from imaging genetics. Biol Psychol. 79:9–22.
Meyer-Lindenberg A. 2010. Imaging genetics of schizophrenia. Dialogues Clin Neurosci. 12:449–456.
Micheloyannis S, Pachou E, Stam CJ, Breakspear M, Bitsios P, Vourkas M, Erimaki S, Zervakis M. 2006. Small-world networks and disturbed functional connectivity in schizophrenia. Schizophr Res. 87:60–66.
Mori S, Kaufmann WE, Davatzikos C, Stieltjes B, Amodei L, Fredericksen K, Pearlson GD, Melhem ER, Solaiyappan M, Raymond GV *et al*. 2002. Imaging cortical association tracts in the human brain using diffusion-tensor-based axonal tracking. Magn Reson Med. 47:215–223.
Mori S, Zhang J. 2006. Principles of diffusion tensor imaging and its applications to basic neuroscience research. Neuron. 51:527–539.
Qu M, Tang F, Yue W, Ruan Y, Lu T, Liu Z, Zhang H, Han Y, Zhang D, Wang F. 2007. Positive association of the disrupted-in-schizophrenia-1 gene (DISC1) with schizophrenia in the Chinese Han population. Am J Med Genet B Neuropsychiatr Genet. 144B:266–270.
Shu N, Liu Y, Li J, Li Y, Yu C, Jiang T. 2009. Altered anatomical network in early blindness revealed by diffusion tensor tractography. PLoS One. 4:e7228.
Singh KK, De Rienzo G, Drane L, Mao Y, Flood Z, Madison J, Ferreira M, Bergen S, King C, Sklar P *et al*. 2011. Common DISC1 polymorphisms disrupt Wnt/GSK3beta signaling and brain development. Neuron. 72:545–558.
Skudlarski P, Jagannathan K, Anderson K, Stevens MC, Calhoun VD, Skudlarska BA, Pearlson G. 2010. Brain connectivity is not only lower but different in schizophrenia: a combined anatomical and functional approach. Biol Psychiatry. 68:61–69.
Sprooten E, Sussmann JE, Moorhead TW, Whalley HC, Ffrench-Constant C, Blumberg HP, Bastin ME, Hall J, Lawrie SM, McIntosh AM. 2011. Association of white matter integrity with genetic variation in an exonic DISC1 SNP. Mol Psychiatry. 16:685; 688–689.
Strogatz SH. 2001. Exploring complex networks. Nature. 410:268–276.
Sussmann JE, Lymer GK, McKirdy J, Moorhead TW, Munoz Maniega S, Job D, Hall J, Bastin ME, Johnstone EC, Lawrie SM *et al*. 2009. White matter abnormalities in bipolar disorder and schizophrenia detected using diffusion tensor magnetic resonance imaging. Bipolar Disord. 11:11–18.
Thomas G, Sinville R, Sutton S, Farquar H, Hammer RP, Soper SA, Cheng YW, Barany F. 2004. Capillary and microelectrophoretic separations of ligase detection reaction products produced from low-abundant point mutations in genomic DNA. Electrophoresis. 25:1668–1677.
Tzourio-Mazoyer N, Landeau B, Papathanassiou D, Crivello F, Etard O, Delcroix N, Mazoyer B, Joliot M. 2002. Automated anatomical labeling of activations in SPM using a macroscopic anatomical parcellation of the MNI MRI single-subject brain. Neuroimage. 15:273–289.
van den Heuvel MP, Mandl RC, Stam CJ, Kahn RS, Hulshoff Pol HE. 2010. Aberrant frontal and temporal complex network structure in schizophrenia: a graph theoretical analysis. J Neurosci. 30:15915–15926.
Wakana S, Caprihan A, Panzenboeck MM, Fallon JH, Perry M, Gollub RL, Hua K, Zhang J, Jiang H, Dubey P *et al*. 2007. Reproducibility of quantitative tractography methods applied to cerebral white matter. Neuroimage. 36:630–644.
Wakana S, Jiang H, Nagae-Poetscher LM, van Zijl PC, Mori S. 2004. Fiber tract-based atlas of human white matter anatomy. Radiology. 230:77–87.
Wang Q, Su TP, Zhou Y, Chou KH, Chen IY, Jiang T, Lin CP. 2012. Anatomical insights into disrupted small-world networks in schizophrenia. Neuroimage. 59:1085–1093.
Watts DJ, Strogatz SH. 1998. Collective dynamics of 'small-world' networks. Nature. 393:440–442.
Witelson SF. 1989. Hand and sex differences in the isthmus and genu of the human corpus callosum. A postmortem morphological study. Brain. 112 (Pt 3):799–835.
Wood JD, Bonath F, Kumar S, Ross CA, Cunliffe VT. 2009. Disrupted-in-schizophrenia 1 and neuregulin 1 are required for the specification of oligodendrocytes and neurones in the zebrafish brain. Hum Mol Genet. 18:391–404.
Yi P, Chen Z, Zhao Y, Guo J, Fu H, Zhou Y, Yu L, Li L. 2009. PCR/LDR/capillary electrophoresis for detection of single-nucleotide differences between fetal and maternal DNA in maternal plasma. Prenat Diagn. 29:217–222.
Zalesky A, Fornito A, Seal ML, Cocchi L, Westin CF, Bullmore ET, Egan GF, Pantelis C. 2011. Disrupted axonal fiber connectivity in schizophrenia. Biol Psychiatry. 69:80–89.